Physics Letters B 784 (2018) 392–396

Contents lists available at ScienceDirect

Physics Letters B

www.elsevier.com/locate/physletb

Spectroscopy of $^{65,67}_{25}$Mn: Strong coupling in the $N = 40$ "island of inversion"

X.Y. Liu [a,b], Z. Liu [a,*], B. Ding [a,*], P. Doornenbal [c], A. Obertelli [c,d,e], S.M. Lenzi [f], P.M. Walker [g], L.X. Chung [h], B.D. Linh [h], G. Authelet [d], H. Baba [c], D. Calvet [d], F. Château [d], A. Corsi [d], A. Delbart [d], J.-M. Gheller [d], A. Gillibert [d], T. Isobe [c], V. Lapoux [d], M. Matsushita [i], S. Momiyama [c,j], T. Motobayashi [c], M. Niikura [j], F. Nowacki [k], H. Otsu [c], C. Péron [d], A. Peyaud [d], E.C. Pollacco [d], J.-Y. Roussé [d], H. Sakurai [c,j], M. Sasano [c], Y. Shiga [c,l], S. Takeuchi [c], R. Taniuchi [c,j], T. Uesaka [c], H. Wang [c], K. Yoneda [c], Y.H. Lam [a], T.H. Huang [a], M.D. Sun [a,b], W.Q. Zhang [a,b], H.Y. Lu [a,b], D.S. Hou [a,b], F. Browne [m], Zs. Dombradi [n], S. Franchoo [o], F. Giacoppo [p], A. Gottardo [o], K. Hadynska-Klek [p], Z. Korkulu [n], S. Koyama [c,j], Y. Kubota [c,i], J. Lee [q], M. Lettmann [e], R. Lozeva [k,r], K. Matsui [c,j], T. Miyazaki [c,j], S. Nishimura [c], C. Louchart [e], L. Olivier [o], S. Ota [i], Z. Patel [g], E. Sahin [p], C. Santamaria [d,c], C. Shand [g], P.-A. Söderström [c], G.L. Stefan [o], D. Steppenbeck [i], T. Sumikama [s], D. Suzuki [o], Zs. Vajta [n], V. Werner [e], J. Wu [c,t], Z. Xu [q], X.H. Zhou [a], Y.H. Zhang [a], H.S. Xu [a], F.S. Zhang [u,v]

[a] Joint Research Center for Modern Physics and Clean Energy, South China Normal University, Institute of Modern Physics of CAS; CAS Key Laboratory of High Precision Nuclear Spectroscopy, Institute of Modern Physics, Chinese Academy of Sciences, Lanzhou 730000, China
[b] University of Chinese Academy of Sciences, Beijing 100049, China
[c] RIKEN Nishina Center, 2-1 Hirosawa, Wako, Saitama 351-0198, Japan
[d] IRFU, CEA, Université Paris-Saclay, F-91191 Gif-sur-Yvette, France
[e] Institut für Kernphysik, Technische Universität Darmstadt, 64289 Darmstadt, Germany
[f] Universitá di Padova and INFN, Sezione di Padova, I-35131 Padova, Italy
[g] Department of Physics, University of Surrey, Guildford GU2 7XH, United Kingdom
[h] Institute for Nuclear Science & Technology, VINATOM, 179 Hoang Quoc Viet, Cau Giay, Hanoi, Viet Nam
[i] Center for Nuclear Study, University of Tokyo, RIKEN campus, Wako, Saitama 351-0198, Japan
[j] Department of Physics, University of Tokyo, 7-3-1 Hongo, Bunkyo, Tokyo 113-0033, Japan
[k] IPHC, CNRS/IN2P3, Université de Strasbourg, F-67037 Strasbourg, France
[l] Department of Physics, Rikkyo University, 3-34-1 Nishi-Ikebukuro, Toshima, Tokyo 172-8501, Japan
[m] School of Computing Engineering and Mathematics, University of Brighton, Brighton BN2 4GJ, United Kingdom
[n] MTA Atomki, P.O. Box 51, Debrecen H-4001, Hungary
[o] Institut de Physique Nucléaire Orsay, IN2P3-CNRS, 91406 Orsay Cedex, France
[p] Department of Physics, University of Oslo, N-0316 Oslo, Norway
[q] Department of Physics, The University of Hong Kong, Pokfulam, Hong Kong
[r] CSNSM, CNRS/IN2P3, Université Paris-Saclay, F-91405 Orsay Campus, France
[s] Department of Physics, Tohoku University, Sendai 980-8578, Japan
[t] State Key Laboratory of Nuclear Physics and Technology, Peking University, Beijing 100871, PR China
[u] Key Laboratory of Beam Technology and Material Modification of Ministry of Education, College of Nuclear Science and Technology, Beijing Normal University, Beijing 100875, China
[v] Beijing Radiation Center, Beijing 100875, China

ARTICLE INFO

Article history:
Received 16 April 2018
Received in revised form 19 June 2018
Accepted 29 June 2018
Available online 3 July 2018

ABSTRACT

Excited states in ^{63,65,67}Mn were studied via in-beam γ-ray spectroscopy following knockout reactions from ^{68}Fe. Similar level schemes, consisting of the $11/2^-$, $9/2^-$, $7/2^-$ and $5/2^-_{g.s.}$ level sequence, connected by $I \rightarrow I-1$ transitions, were established, the first time for ^{65,67}Mn. Their level structures show features consistent with strongly-coupled rotational bands with $K = 5/2$. State-of-the-art shell-model calculations with the modified LNPS effective interaction reproduce the observed levels remarkably

* Corresponding authors.
E-mail addresses: liuzhong@impcas.ac.cn (Z. Liu), dbing@impcas.ac.cn (B. Ding).

https://doi.org/10.1016/j.physletb.2018.06.067

Editor: V. Metag

Keywords:
In-beam γ-ray spectroscopy
"Island of inversion" around $N = 40$
Strong coupling
Structure evolution

well and suggest the dominance of 4-particle-4-hole neutron configurations for all the states. The data on the low-lying excited states of odd-mass $^{53-67}$Mn provide a textbook example of nuclear structure evolution from weak coupling through decoupling to strong coupling along a single isotopic chain on the n-rich side of the β stability line. These results help to deepen our understanding of the $N = 40$ "island of inversion".

1. Introduction

With the acquisition of experimental data on nuclei far from stability in the last decades, the paradigm of universal shell structure has been abandoned [1,2], and much progress has been made by investigating the mechanism of shell evolution. At the $N = 40$ harmonic oscillator shell closure, ^{68}Ni has the appearance of doubly magic based on the high 2_1^+ energy [3] and low transition probability to the ground state [4,5]. However, the strength of this $N = 40$ shell closure was later proved to be unexpectedly weak by mass measurements [6,7]. While its ground state is still dominated by the normal fp configuration of a spherical shape [8–10], well deformed structures that become the ground state of lighter $N \sim 40$ nuclei have been observed recently, especially in Fe and Cr isotopes [11–17]. The experimental results available for these nuclei have been interpreted within the shell model framework in a large model space that includes the key orbitals, $\nu 1g_{9/2}$ and $\nu 2d_{5/2}$, for the development of quadrupole deformation [19]. Similar to the neutron-rich region around $N = 20$, where the ground state wave functions are dominated by intruder configurations, this area has been described as a new "island of inversion" [14,18,19]. Indeed, the occurrence of intruder deformed configurations is attributed to both monopole effects due to the migration of neutron single-particle states as protons are removed from the $\pi 1f_{7/2}$ orbital [20,21] and multipole effects that favor quadrupole correlations in this valence space [19,22].

The collective properties in this region were obtained mainly from the study of even-even nuclei, while spectroscopic information on the odd-mass nuclei is still scarce due to the higher level density and the diversity of level structures even at low excitation energies. Compared with the relatively simple response of even-even nuclei to the development of collectivity, e.g., the decrease of the 2_1^+ energy and the increase of the $E(4_1^+)/E(2_1^+)$ ratio, the level structure of an odd-mass nucleus is sensitive to both the deformation of the underlying even-even core and the configuration of the unpaired nucleon [23]. Odd-mass nuclei therefore provide key additional insights into the nuclear structure evolution. Depending on the shape of the core and the strength of the Coriolis interaction [24], level and decay patterns corresponding to three distinct coupling-scheme limits can be recognized: weak coupling, decoupling and strong coupling [25]. For example at $Z = 27$, where the even-N Co isotopes have been studied up to $A = 67$, the low-lying states in odd-A Co isotopes can be understood in terms of weak coupling, indicating the dominance of single particle excitations around the semi-magic Ni isotopes [26]. On the other hand, the observation of deformed structures at low excitation energy in ^{67}Co implies the proximity to the edge of the "island of inversion" around $N = 40$.

Lying in between Cr and Fe, Mn isotopes are expected to be well deformed around $N = 40$, so it is very intriguing and challenging to reveal the particle-core coupling mode in these odd-mass Mn isotopes. Comprehensive investigations of the excited states in Mn isotopes with $N < 40$ have been carried out in various experiments. High-spin states in $^{57-60}$Mn have been studied using fusion-evaporation reactions [27]. In-beam γ spectroscopy of $^{59-63}$Mn has been carried out via multi-nucleon transfer reactions [28]. Recently, excited states up to $11/2^-$ in ^{63}Mn have been established in the fragmentation of ^{65}Fe [29], and ground state properties of $^{53-63}$Mn have been determined by laser spectroscopy at ISOLDE [30–32]. So far, except an unassigned 272 keV γ-ray observed in ^{65}Mn [33], γ-ray spectroscopy of Mn isotopes with $N \geq 40$ has been out of experimental reach. In this Letter, we report on the first observation of excited states in ^{65,67}Mn and the confirmation of the ^{63}Mn result reported recently [29]. The level structures of ^{65,67}Mn display features of strongly-coupled rotational bands expected for well deformed odd-A nuclei. The nuclear structure evolution along the Mn isotopic chain ($N = 28$–42) from weak coupling through decoupling to strong coupling are discussed. In addition, as key isotopes in Urca cycle that cools the neutron star crusts via neutrino cooling [34], information on the low-lying levels of ^{63,65}Mn are of importance in deducing the electron capture and β-decay rates for the ^{63}Fe $\leftrightarrow$ ^{63}Mn and ^{65}Fe $\leftrightarrow$ ^{65}Mn Urca pairs [34].

2. Experiment and results

The experiment was performed at the Radioactive Isotope Beam Factory (RIBF), operated by the RIKEN Nishina Center and the Center for Nuclear Study of the University of Tokyo. A 15 pnA ^{238}U primary beam, accelerated to 345 MeV/u, was impinged on a 3-mm-thick ^{9}Be primary target for the production of secondary radioactive isotope beams via in-flight fission reactions at the entrance of the BigRIPS separator [35]. The isotopes of interest were selected and separated from intense secondary beams through the $B\rho$–ΔE–$B\rho$ method [36], and then impinged on a 102(1)-mm-thick liquid hydrogen (LH_2) secondary target at an incident energy of about 260 MeV/u. The secondary reaction residues were produced via proton-induced knockout reactions. The particle identification before and after the LH_2 target was performed unambiguously by the $B\rho$–ΔE–ToF method event-by-event in the BigRIPS and ZeroDegree spectrometer [36], respectively. The Time-Projection Chamber (TPC) of the MINOS device [37] surrounding the LH_2 target was used to reconstruct the vertex of the knockout reactions by tracking the emitted protons. The γ rays emitted in-flight were measured by the DALI2 γ-ray spectrometer [38] surrounding the MINOS device. The setup is identical to previous experiments at the RIBF [17,39–44].

In the present work, excited states of ^{63,65,67}Mn were populated by the fragmentation of ^{68}Fe via the ^{68}Fe$(p, 2pxn)^{67-x}$Mn reaction channels, with $x = 4$, 2 and 0, respectively. The Doppler-corrected γ-ray spectra are displayed in Fig. 1, where the response functions of DALI2 were simulated with the GEANT4 framework [45] and the background was composed of two Landau functions. Three transitions were identified in the singles spectrum for each isotope. The information on the observed γ-transitions is summarized in Table 1. The effect on transition energy of the lifetime for the initial state has been evaluated and found to be negligible. The level schemes, displayed in Fig. 2, were established based on the γ–γ coincidence relationships and the relative intensities from both the singles and coincidence spectra. The spin-parity assign-

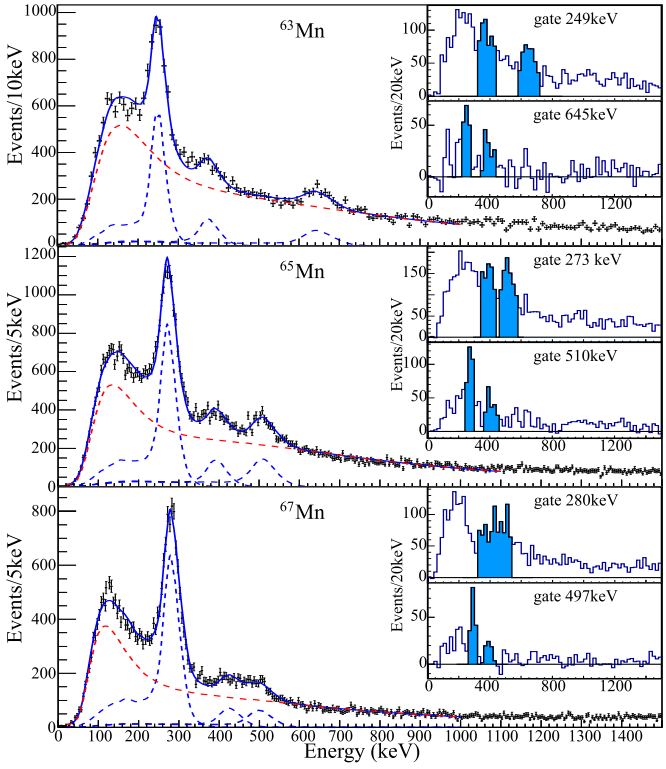

Fig. 1. (Color online.) Doppler-corrected γ-ray spectra of ^{63,65,67}Mn detected by DALI2, and the background subtracted γ–γ coincidence spectra labeled with the gating transitions are displayed in the insets.

Table 1
The γ-transition energies (E_γ), relative intensities after efficiency calibration (I_γ) observed in ^{63,65,67}Mn, and the tentative spin-parity assignments of the initial and final states.

Isotope	$J_i^\pi \rightarrow J_f^\pi$	E_γ (keV)	I_γ
^{63}Mn	$(7/2^-) \rightarrow 5/2^-_{g.s.}$	249(5)	100(4)
	$(9/2^-) \rightarrow (7/2^-)$	645(6)	20(2)
	$(11/2^-) \rightarrow (9/2^-)$	376(7)	20(2)
^{65}Mn	$(7/2^-) \rightarrow (5/2^-_{g.s.})$	273(5)	100(2)
	$(9/2^-) \rightarrow (7/2^-)$	510(6)	22(1)
	$(11/2^-) \rightarrow (9/2^-)$	394(6)	16(1)
^{67}Mn	$(7/2^-) \rightarrow (5/2^-_{g.s.})$	280(5)	100(2)
	$(9/2^-) \rightarrow (7/2^-)$	497(7)	13(1)
	$(11/2^-) \rightarrow (9/2^-)$	427(8)	11(1)

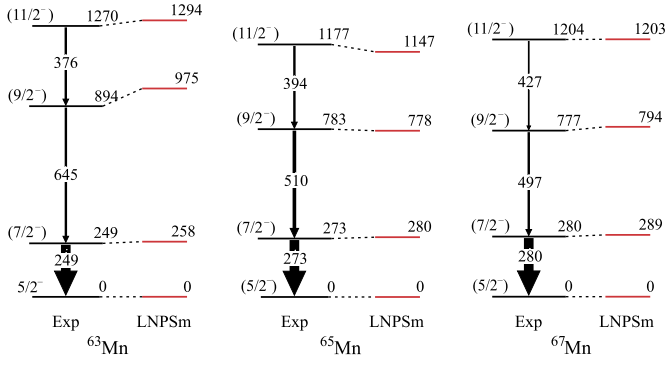

Fig. 2. (Color online.) Experimental level schemes (black solid line) of ^{63,65,67}Mn in comparison with the large-scale shell-model calculations (red solid line).

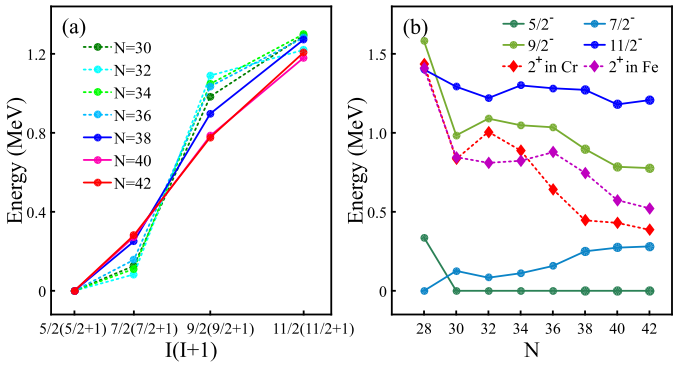

Fig. 3. Structural evolution in the Mn isotopic chain. (a) Experimental excitation energies of low-lying yrast states in even-N Mn isotopes as a function of $I(I+1)$. (b) The systematics of low-lying level energies in odd-A Mn isotopes and $E(2_1^+)$ in even-A Ni, Fe and Cr isotopes [56]. The data of ^{63,65,67}Mn are from the present work. (For interpretation of the colors in the figure(s), the reader is referred to the web version of this article.)

ments were made following the systematics of low-lying levels in the lighter odd-mass Mn isotopes (see Fig. 3 (b)) as well as shell-model calculations as described below. It is worth noting that the population of $11/2^-$ level in ^{67}Mn, corresponding to one proton removal from ^{68}Fe, is hard to be explained by one-step direct reaction, and may indicate a non-sudden dissipative process [46] or ^{68}Fe$(p,p)^{68}$Fe$^{2+}(p,2p)^{67}$Mn multi-step reaction in the thick LH_2 target.

In this work, large-scale shell-model calculations for ^{63,65,67}Mn were performed using the modified LNPS [19] effective interaction (LNPSm) and the M-scheme shell-model code ANTOINE [47]. The defined model space is based on a ^{48}Ca closed core consisting of the full fp shell for the valence protons and the $1p_{3/2}$, $1p_{1/2}$, $0f_{5/2}$, $0g_{9/2}$ and $1d_{5/2}$ orbits for valence neutrons. The interaction of original LNPS is a mixture of several sets of realistic two-body matrix elements [19], and the quadrupole–quadrupole interaction of the neutron $0g_{9/2}$ and $1d_{5/2}$ orbits were increased to compensate the absence of $2p_{1/2}$ neutron orbit. The interaction used here is different from the original LNPS, minor modification on the monopole and pairing parts of the effective Hamiltonian were applied in order to describe a broader region [17]. Based on this modified LNPS effective interaction (LNPSm), the observed levels were reproduced remarkably well with a maximum energy deviation of 81 keV for the $9/2^-$ level in ^{63}Mn, better than 163 keV, the result of LNPS interaction [29].

3. Discussion

The level schemes of ^{63,65,67}Mn are very similar, consisting of the $11/2^-$, $9/2^-$, $7/2^-$ and $5/2^-_{g.s.}$ level sequence, connected by $\Delta I = 1$ transitions. The experimental excitation energies of the yrast states up to $11/2^-$ in odd-A Mn isotopes from $N = 30$ to 42 are plotted in Fig. 3 (a) as a function of $I(I+1)$. With the nearly linear relationship for $N = 40$ and 42 (see Fig. 3 (a)), akin to ideal rotors [23] and the dominance of $\Delta I = 1$ transitions observed, the levels in ^{65,67}Mn manifest typical characteristics of strongly coupled bands with band-head spin of $j = K = 5/2$. As for ^{63}Mn, a transitional feature between decoupling and strong coupling is reflected in the slight departure from the linear relation in excitation energy. In Mn isotopes heavier than ^{63}Mn, the signature staggering gets smaller but still remains. This can possibly be attributed to the triaxial deformation and/or softness in the potential energy surface as suggested in the Monte-Carlo Shell Model calculations [48] and the Hartree–Fock–Bogoliubov approximation [49].

Table 2
The shell-model reduced transition probabilities $B(M1)$ (μ_N^2) and $B(E2)$ ($e^2\,fm^4$). The intrinsic quadrupole moments Q_0 ($e\,fm^2$) and β_2 values of their respective initial states extracted from the $B(E2)$ values with $K = 5/2$.

$J_i^\pi \rightarrow J_f^\pi$	^{63}Mn				^{65}Mn				^{67}Mn			
	$B(M1)$	$B(E2)$	Q_0	$\langle\beta_2\rangle$	$B(M1)$	$B(E2)$	Q_0	$\langle\beta_2\rangle$	$B(M1)$	$B(E2)$	Q_0	$\langle\beta_2\rangle$
$7/2^- \rightarrow 5/2^-$	0.16	497	119	0.28	0.33	608	131	0.30	0.30	631	134	0.30
$9/2^- \rightarrow 5/2^-$	/	115	108	0.26	/	175	132	0.30	/	182	135	0.30
$9/2^- \rightarrow 7/2^-$	0.33	359	110	0.28	0.57	480	127	0.29	0.46	506	130	0.29
$11/2^- \rightarrow 7/2^-$	/	297	132	0.31	/	302	133	0.30	/	316	136	0.30
$11/2^- \rightarrow 9/2^-$	0.61	277	110	0.28	0.85	382	129	0.29	0.68	389	130	0.29

The systematics of low-lying levels along the Mn isotopic chain from $N = 28$ to 42 is shown in Fig. 3 (b). The behavior of these isotopes can be explained in terms of the particle-core coupling in an evolutionary view with the increase of deformation. In the semi-magic ^{53}Mn [50], with a $7/2^-$ ground state, the $9/2^-$ and $11/2^-$ states cluster around the 2_1^+ of ^{52}Cr [51] in energy, can be interpreted as the weak coupling of a $\pi 1f_{7/2}$ particle to the 2_1^+ of ^{52}Cr. From ^{55}Mn to ^{61}Mn, the ground states are $5/2^-$ and become moderately deformed ($\beta_2 \approx 0.25$) [32], the $9/2^-$ levels follow the 2_1^+ in Cr or Fe isotones in energy, the $R_{j+4/j+2}$ ($E(13/2_1^-)/E(9/2_1^-)$) ratios are about the same as the $R_{4/2}$ of their even-even cores, and $\Delta I = 2$ $E2$ transitions are much stronger, exhibiting the feature of decoupling [25]. In ^{65,67}Mn the level structures evolve into strong coupling with the level energies following the $I(I+1)$ law and the decay patterns dominated by $\Delta I = 1$ transitions.

To corroborate the observed dominance of $I \rightarrow (I-1)$ transitions in the level decay pattern, reduced transition probabilities $B(M1)$ and $B(E2)$ were calculated with effective charges $e_\pi = 1.31$ and $e_\nu = 0.46$ and listed in Table 2. Using the experimental transition energies and the theoretical $B(M1)$ and $B(E2)$ values, the branching ratios for the $9/2^- \rightarrow 5/2^-_{g.s.}$ transitions relative to the $9/2^- \rightarrow 7/2^-$ ones were estimated to be 6%, 4%, and 6% for ^{63,65,67}Mn, respectively. These cross-over transitions are too weak to be detected by the present setup. Similarly, the branching ratios for $11/2^- \rightarrow 7/2^-$ relative to the $11/2^- \rightarrow 9/2^-$ transition were calculated to be 71%, 24% and 28%, consistent with the upper limits of 65%, 23% and 33% extracted from the singles spectra at a 95% confidence level.

Based on the rotational model, the intrinsic quadrupole moments and the β_2 values listed in Table 2 were obtained from the calculated $B(E2)$ values [55]. Tested with all possible K values, only the calculations using $K = 5/2$ produce substantial and nearly constant intrinsic quadrupole moments for all the observed excited states, consistent with the spin and configuration assignments presented above. The β_2 values deduced are about 0.3, falling between the theoretical predictions for the Cr (0.33) and Fe (0.29) isotopes in this region [17] but less than the quadrupole deformation of 0.35(3) deduced for ^{63}Mn in laser spectroscopy [32]. The quadrupole moment measurement of ^{63,65,67}Mn in future experiments will be essential in further testing of the shell-model calculation.

Proton and neutron occupation numbers for the yrast states up to $11/2^-$ in ^{63,65,67}Mn were calculated with the shell model. The proton occupation numbers are nearly constant in these three Mn isotopes, there is about 1 proton has been excited cross $Z = 28$ shell to the $\pi 2p_{3/2}$ and $\pi 1f_{5/2}$ orbits. The wave function of these low-lying states in valence neutron are dominated by $4p-4h$ neutron excitations from the pf shell into the $\nu 1g_{9/2}$ and $\nu 2d_{5/2}$ orbits, and the number of excited neutrons from the pf shell reaches a maximum at $N = 40$. The orbital occupations are consistent with the collectivity being mainly generated by quadrupole correlations between protons and neutrons in Quasi-SU3 and Pseudo-SU3 model spaces [52–54].

4. Conclusion

In summary, we studied the low-lying level structures of ^{63,65,67}Mn, the first time for the latter two. Very similar level schemes with $11/2^- \rightarrow 9/2^- \rightarrow 7/2^- \rightarrow 5/2^-_{g.s.}$ transition cascades were established. With the excitation energies closely proportional with $I(I+1)$ and the decay pattern dominated by $\Delta I = 1$ transitions, the first cases of strongly-coupled rotational bands in the $N = 40$ "island of inversion" have been identified in ^{65,67}Mn. Large-scale shell-model calculations using the LNPSm effective interaction reproduce the observed excitation energies and decay patterns very well, also supporting the $K = 5/2$ configuration proposed for the rotational structures. In addition to the neutron $4p-4h$ configuration, the proton $1p-1h$ cross-shell excitations are predicted in ^{63,65,67}Mn. With the data obtained in the present work, the low-lying level systematics along the Mn isotopic chain from $N = 28$ to 42 provide a textbook example of nuclear structure evolution from weak coupling through decoupling to strong coupling on the n-rich side of the chart of nuclides.

Acknowledgements

The work at Institute of Modern Physics was supported by the National Natural Science Foundation of China (Grant Nos. 11635003, 11675225, 11405224, U1632144 and 11435014), the National Key R&D Program of China (Contract No. 2018YFA0404400), the Hundred Talented Project of the Chinese Academy of Sciences and the Key Research Program of the Chinese Academy of Sciences (Grant No. XDPB09). We express our gratitude to the RIKEN Nishina Center accelerator staff for providing the stable and high-intensity uranium beam and to the BigRIPS team for operating the secondary beams. The development of MINOS and the core MINOS team were supported by the European Research Council through the ERC Grant No. MINOS-258567. All UK authors are supported by STFC. L.X. Chung and B.D. Linh are supported by Ministry of Science and Technology under Grant Nos. ĐTCB 09/17/VKHKTHN and ĐTĐLCN.25/18. The Hungarian authors are supported by the GINOP-2.3.3-15-2016-00034 project. This project is supported by the national key research and development program (MOST 2016YFA0400501). BMBF Grant Nos. 05P15RDFN1 and 05P12RDFN8 for TU Darmstadt people. The support to X.Y. Liu provided by China Scholarship Council (No. 201700260183) during the visit to Sweden is acknowledged.

Helpful discussions with J. Meng, Y. Sun, B. Cederwall, C. Qi, H. Jin and F.R. Xu are appreciated.

References

[1] O. Sorlin, M.-G. Porquet, Prog. Part. Nucl. Phys. 61 (2008) 602.
[2] D. Steppenbeck, et al., Nature (London) 502 (2013) 207.
[3] R. Broda, et al., Phys. Rev. Lett. 74 (1995) 868.
[4] F. Azaiez, Phys. Scr. T 88 (2000) 118.
[5] O. Sorlin, et al., Phys. Rev. Lett. 88 (2002) 092501.
[6] C. Guenaut, et al., Phys. Rev. C 75 (2007) 044303.
[7] S. Rahaman, et al., Eur. Phys. J. A 34 (2007) 5.

[8] S. Suchyta, et al., Phys. Rev. C 89 (2014), 021301(R).
[9] F. Flavigny, et al., Phys. Rev. C 91 (2015) 034310.
[10] B.P. Crider, et al., Phys. Lett. B 736 (2016) 108.
[11] M. Hannawald, et al., Phys. Rev. Lett. 82 (1999) 1391.
[12] O. Sorlin, et al., Eur. Phys. J. A 16 (2003) 55.
[13] S. Lunardi, et al., Phys. Rev. C 76 (2007) 034303.
[14] P. Adrich, et al., Phys. Rev. C 77 (2008) 054306.
[15] A. Gade, et al., Phys. Rev. C 81 (2010), 051304(R).
[16] H.L. Crawford, et al., Phys. Rev. Lett. 110 (2013) 242701.
[17] C. Santamaria, et al., Phys. Rev. Lett. 115 (2015) 192501.
[18] J. Ljungvall, et al., Phys. Rev. C 81 (2010), 061301(R).
[19] S.M. Lenzi, et al., Phys. Rev. C 82 (2010) 054301.
[20] T. Otsuka, et al., Phys. Rev. Lett. 95 (2005) 232502.
[21] N. Smirnova, et al., Phys. Lett. B 686 (2010) 109.
[22] E. Caurier, et al., Eur. Phys. J. A 15 (2002) 145.
[23] R.F. Casten, Nuclear Structure From a Simple Perspective, Oxford University, New York, 2000 (Chaps. 8).
[24] F.S. Stephens, Rev. Mod. Phys. 47 (47) (1975) 43–65.
[25] D. Bucurescu, N.V. Zamfir, Phys. Rev. C 95 (2017) 014329.
[26] F. Recchia, et al., Phys. Rev. C 85 (2012) 064305.
[27] D. Steppenbeck, et al., Phys. Rev. C 81 (2010) 014305.
[28] J.J. Valiente-Dobon, et al., Phys. Rev. C 78 (2008) 024302.
[29] T. Baugher, et al., Phys. Rev. C 93 (2016) 014313.
[30] C. Babcock, et al., Phys. Lett. B 750 (2015) 176.
[31] H. Heylen, et al., Phys. Rev. C 92 (2015) 044311.
[32] C. Babcock, et al., Phys. Lett. B 760 (2016) 387.
[33] L. Gaudefroy, et al., Eur. Phys. J. A 23 (2005) 41.
[34] H. Schatz, et al., Nature 505 (2014) 62.
[35] T. Kubo, et al., Prog. Theor. Exp. Phys. (2012) 03C003.
[36] N. Fukuda, et al., Nucl. Instrum. Methods Phys. Res., Sect. B 317 (2013) 323.
[37] A. Obertelli, et al., Eur. Phys. J. A 50 (2014) 8.
[38] S. Takeuchi, et al., Nucl. Instrum. Methods Phys. Res., Sect. A 763 (2014) 596.
[39] L. Olivier, et al., Phys. Rev. Lett. 119 (2017) 192501.
[40] M. Lettman, et al., Phys. Rev. C 96 (2017), 011301(R).
[41] N. Paul, et al., Phys. Rev. Lett. 118 (2017) 032501.
[42] F. Flavigny, et al., Phys. Rev. Lett. 118 (2017) 242501.
[43] S. Chen, et al., Phys. Rev. C 95 (2017), 041302(R).
[44] C.M. Shand, et al., Phys. Lett. B 773 (2017) 492.
[45] S. Agostinelli, et al., Nucl. Instrum. Methods Phys. Res. A 506 (2003) 250.
[46] F. Flavigny, et al., Phys. Rev. Lett. 108 (2012) 252501.
[47] E. Caurier, et al., Acta Phys. Pol. B 30 (1999) 705.
[48] H. Heylen, et al., Phys. Rev. C 94 (2016) 054321.
[49] K. Sato, et al., Phys. Rev. C 86 (2012) 024316.
[50] J.R. Brown, et al., Phys. Rev. C 80 (2009), 011306(R).
[51] R. Kumar, et al., Phys. Rev. C 76 (2007) 034301.
[52] A.P. Zuker, et al., Phys. Rev. C 52 (1995) R1744.
[53] A.P. Zuker, A. Poves, F. Nowacki, S.M. Lenzi, Phys. Rev. C 92 (2015) 024320.
[54] T. Braunroth, et al., Phys. Rev. C 92 (2015) 034306.
[55] B.V. Pritychenko, et al., Phys. Rev. C 63 (2001) 011305.
[56] www.nndc.bnl.gov.